

Applied Mathematical Sciences, Vol. 6, 2012, no. 129, 6425 - 6436

Analysis of Maximum Likelihood Classification on Multispectral Data

Asmala Ahmad

Department of Industrial Computing
Faculty of Information and Communication Technology
Universiti Teknikal Malaysia Melaka
Hang Tuah Jaya, 76100 Durian Tunggal, Melaka, Malaysia
asmala@utem.edu.my

Shaun Quegan

School of Mathematics and Statistics
University of Sheffield
Sheffield, United Kingdom

Abstract

The aim of this paper is to carry out analysis of Maximum Likelihood (ML) classification on multispectral data by means of qualitative and quantitative approaches. ML is a supervised classification method which is based on the Bayes theorem. It makes use of a discriminant function to assign pixel to the class with the highest likelihood. Class mean vector and covariance matrix are the key inputs to the function and can be estimated from the training pixels of a particular class. In this study, we used ML to classify a diverse tropical land covers recorded from Landsat 5 TM satellite. The classification is carefully examined using visual analysis, classification accuracy, band correlation and decision boundary. The results show that the separation between mean of the classes in the decision space is to be the main factor that leads to the high classification accuracy of ML.

Keywords: ML, Classification, Decision Boundary

1 Introduction

Maximum Likelihood (ML) is a supervised classification method derived from the Bayes theorem, which states that the a posteriori distribution $P(i|\omega)$, i.e., the probability that a pixel with feature vector ω belongs to class i , is given by:

$$P(i|\omega) = \frac{P(\omega|i)P(i)}{P(\omega)} \quad (1)$$

where $P(\omega|i)$ is the likelihood function, $P(i)$ is the a priori information, i.e., the probability that class i occurs in the study area and $P(\omega)$ is the probability that ω is observed, which can be written as:

$$P(\omega) = \sum_{i=1}^M P(\omega|i)P(i) \quad (2)$$

where M is the number of classes. $P(\omega)$ is often treated as a normalisation constant to ensure $\sum_{i=1}^M P(i|\omega)$ sums to 1. Pixel x is assigned to class i by the rule:

$$x \in i \quad \text{if } P(i|\omega) > P(j|\omega) \quad \text{for all } j \neq i \quad (3)$$

ML often assumes that the distribution of the data within a given class i obeys a multivariate Gaussian distribution. It is then convenient to define the log likelihood (or discriminant function):

$$g_i(\omega) = \ln P(\omega|i) = -\frac{1}{2}(\omega - \mu_i)^t C_i^{-1}(\omega - \mu_i) - \frac{N}{2} \ln(2\pi) - \frac{1}{2} \ln(|C_i|) \quad (4)$$

Since log is a monotonic function, Equation (3) is equivalent to:

$$x \in i \quad \text{if } g_i(\omega) > g_j(\omega) \quad \text{for all } j \neq i. \quad (5)$$

Each pixel is assigned to the class with the highest likelihood or labelled as unclassified if the probability values are all below a threshold set by the user [9]. The general procedures in ML are as follows:

1. The number of land cover types within the study area is determined.
2. The training pixels for each of the desired classes are chosen using land cover information for the study area. For this purpose, the Jeffries-Matusita (JM) distance can be used to measure class separability of the chosen training pixels.

For normally distributed classes, the JM separability measure for two classes, J_{ij} , is defined as follows [4]:

$$J_{ij} = \sqrt{2(1 - e^{-\alpha})} \tag{6}$$

where α is the Bhattacharyya distance and is given by [4]:

$$\alpha = \frac{1}{8}(\boldsymbol{\mu}_i - \boldsymbol{\mu}_j)^t \left[\frac{(C_i + C_j)}{2} \right]^{-1} (\boldsymbol{\mu}_i - \boldsymbol{\mu}_j) + \frac{1}{2} \ln \left(\frac{\left| \frac{C_i + C_j}{2} \right|}{\sqrt{|C_i||C_j|}} \right) \tag{7}$$

J_{ij} ranges from 0 to 2.0, where $J_{ij} > 1.9$ indicates good separability of classes, moderate separability for $1.0 \leq J_{ij} \leq 1.9$ and poor separability for $J_{ij} < 1.0$ [2].

3. The training pixels are then used to estimate the mean vector and covariance matrix of each class.
4. Finally, every pixel in the image is classified into one of the desired land cover types or labelled as unknown.

In ML classification, each class is enclosed in a region in multispectral space where its discriminant function is larger than that of all other classes. These class regions are separated by decision boundaries, where, the decision boundary between class i and j occurs when:

$$g_i(\boldsymbol{\omega}) = g_j(\boldsymbol{\omega}) \tag{8}$$

For multivariate normal distributions, this becomes:

$$\begin{aligned} &-\frac{1}{2}(\boldsymbol{\omega} - \boldsymbol{\mu}_i)^t C_i^{-1} (\boldsymbol{\omega} - \boldsymbol{\mu}_i) - \frac{N}{2} \ln(2\pi) - \frac{1}{2} \ln(|C_i|) - \\ &\left(-\frac{1}{2}(\boldsymbol{\omega} - \boldsymbol{\mu}_j)^t C_j^{-1} (\boldsymbol{\omega} - \boldsymbol{\mu}_j) - \frac{N}{2} \ln(2\pi) - \frac{1}{2} \ln(|C_j|) \right) = 0 \end{aligned} \tag{9}$$

which can be written as:

$$-(\boldsymbol{\omega} - \boldsymbol{\mu}_i)^t C_i^{-1} (\boldsymbol{\omega} - \boldsymbol{\mu}_i) - \ln(|C_i|) + (\boldsymbol{\omega} - \boldsymbol{\mu}_j)^t C_j^{-1} (\boldsymbol{\omega} - \boldsymbol{\mu}_j) + \ln(|C_j|) = 0 \tag{10}$$

This is a quadratic function in N dimensions. Hence, if we consider only two classes, the decision boundaries are conic sections (i.e. parabolas, circles, ellipses or hyperbolas).

2 Methodology

The study area was located in Selangor, Malaysia, covering approximately 840 km² within longitude 101° 10' E to 101°30' E and latitude 2°99' N to 3°15' N (Figure 1). The satellite data come from bands 1 (0.45 – 0.52 μm), 2 (0.52 – 0.60 μm), 3 (0.63 – 0.69 μm), 4 (0.76 – 0.90 μm), 5 (1.55 – 1.75 μm) and 7 (2.08 – 2.35 μm) of Landsat-5 TM dated 11th February 1999. The satellite records surface reflectance with 30 m spatial resolution from a height of 705 km. Prior to any data processing, masking of cloud and its shadow were carried out based on threshold approach [8], [1]. Visual interpretation of the Landsat data (Figure 1(b)) was carried out to identify main land covers within the study area. The task was aided by a reference map (Figure 1(a)), produced in October 1991 by the Malaysian Surveying Department and Malaysian Remote Sensing Agency using ground surveying and SPOT satellite data. 11 main classes were identified, i.e. water, coastal swamp forest, dryland forest, oil palm, rubber, industry, cleared land, urban, sediment plumes, coconut and bare land.



Fig. 1. The study area from (a) the land cover map and (b) the Landsat-5 TM with bands 5 4 and 3 assigned to the red, green and blue channels. Cloud and its shadow are masked in black.

Training areas were established by choosing one or more polygons for each class. Pixels fall within the training area were taken to be the training pixels for a particular class. In order to select a good training area for a class, the important properties taken into consideration are its uniformity and how well they represent the same class throughout the whole image [5]. Class separability of the chosen training pixels were determined by means of the JM distance. Fifty pairs have JM distance between 1.9 and 2.0 indicating good separability, four from 1.0 to 1.9 indicating moderate separability and one less than 1.0 indicating poor separability. The worst separability, possessed by the urban – industry pair (0.947), was expected since both have quite similar spectral characteristics. For each class, these training pixels provide values from which to estimate the mean and covariances of the spectral bands used. These information are to be used by the ML classifier to assign pixels to a particular class.

3 Analysis of ML classification

3.1 Visual Analysis

The outcome of ML classification after assigning the classes with suitable colours, is shown in Figure 2: coastal swamp forest (green), dryland forest (blue), oil palm (yellow), rubber (cyan), cleared land (purple), coconut (maroon), bare land (orange), urban (red), industry (grey), sediment plumes (sea green) and water (white). Clouds and their shadows are masked black. The areas in terms of percentage and square kilometres were also computed; the classes with the largest area are oil palm, cleared land and industry. Although being similar, coastal swamp forest and dryland forest can be clearly seen in the south-west and north-east of the classified image, as indicated by the reference map. Coastal swamp forest covers most of the Island and coastal regions in the south-west of the scene. Most of the dryland forest can be recognised as a large straight-edged region in the north-east. Oil palm and urban dominate the northern and southern parts respectively. Rubber appears as scattered patches that mostly are surrounded by oil palms. Industry can be recognised as patches near the urban areas, especially in the south-west and north-east. Coconut can be seen in the coastal area in the north-west of the image. A quite large area of bare land can be seen in the east, while cleared land can be seen mostly in the north, south and south-east of the image.

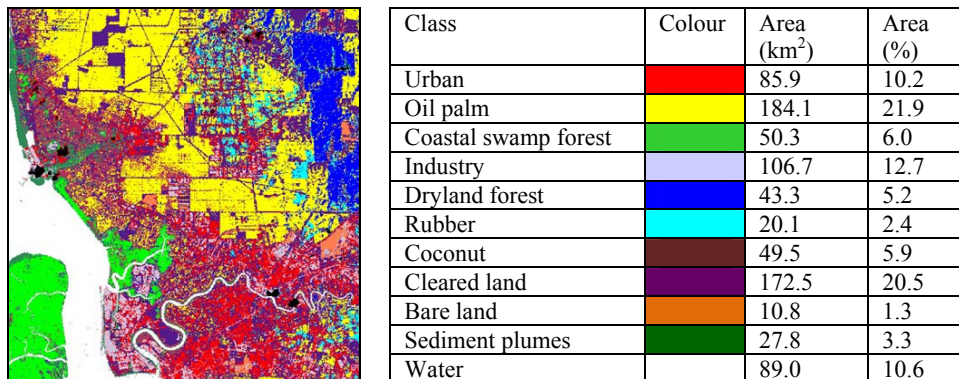


Fig. 2. ML classification using band 1, 2, 3, 4, 5 and 7 of Landsat TM and the class areas in terms of square kilometre and percentage.

3.2 Accuracy Analysis

Accuracy assessment of the ML classification was determined by means of a confusion matrix (sometimes called error matrix), which compares, on a class-by-class basis, the relationship between reference data (ground truth) and the corresponding results of a classification [9]. Such matrices are square, with the number of rows and columns equal to the number of classes, i.e. 11. For all

classes, the numbers of reference pixels are: rubber (103), water (9129), coastal swamp forest (14840), dryland forest (6162), oil palm (10492), industry (350), cleared land (1250), urban (2309), coconut (159), bare land (313) and sediment plumes (1881). The diagonal elements in Table 1(a) represent the pixels of correctly assigned pixels and are also known as the producer accuracy. Producer accuracy is a measure of the accuracy of a particular classification scheme and shows the percentage of a particular ground class that is correctly classified. It is calculated by dividing each of the diagonal elements in Table 1 (a) by the total of each column respectively:

$$\text{Producer accuracy} = \frac{c_{aa}}{c_{\bullet a}} \times 100\% \quad (11)$$

where,

c_{aa} = element at position a^{th} row and a^{th} column

$c_{\bullet a}$ = column sums

The minimum acceptable accuracy for a class is 90% [7]. Table 1(b) shows the producer for all the classes. It is obvious that all classes possess producer accuracy higher than 90%: bare land gives the highest (100%) and oil palm the lowest (92.4%). The relatively low accuracy of oil palm is mainly because 6% and 1% of its pixels were classified as coconut and cleared land. The misclassification of oil palm pixels to the coconut class is due to the fact that oil palm and coconut have a similar physical structure, so tend to have similar spectral behaviour and therefore can easily be misclassified as each other. User Accuracy is a measure of how well the classification is performed. It indicates the percentage of probability that the class which a pixel is classified to on an image actually represents that class on the ground [7]. It is calculated by dividing each of the diagonal elements in a confusion matrix by the total of the row in which it occurs:

$$\text{User accuracy} = \frac{c_{ii}}{c_{i\bullet}} \times 100\% \quad (12)$$

where, $c_{i\bullet}$ = row sum. Coastal swamp forest, dryland forest, oil palm, sediment plumes, water, bare land and urban show a user accuracy of more than 90%. Rubber, cleared land and industry possess accuracy between 70% and 90%, while the worst accuracy is possessed by coconut (16%). The low accuracy of coconut is because the oil palm pixels tend to be classified as coconut because they having similar spectral properties to oil palm. A measure of overall behaviour of the ML classification can be determined by the overall accuracy, which is the total percentage of pixels correctly classified:

$$\text{Overall accuracy} = \frac{\sum_{a=1}^U c_{aa}}{Q} \times 100\% \tag{13}$$

where, Q and U is the total number of pixels and classes respectively. The minimum acceptable overall accuracy is 85% [3]. The Kappa coefficient, κ is a second measure of classification accuracy which incorporates the off-diagonal elements as well as the diagonal terms to give a more robust assessment of accuracy than overall accuracy. It is computed as [6]:

$$\kappa = \frac{\sum_{a=1}^U \frac{c_{aa}}{Q} - \sum_{a=1}^U \frac{c_{a\bullet} \cdot c_{\bullet a}}{Q^2}}{1 - \sum_{a=1}^U \frac{c_{a\bullet} \cdot c_{\bullet a}}{Q^2}} \dots \tag{14}$$

where $c_{a\bullet}$ = row sums. The ML classification yielded an overall accuracy of 97.4% and kappa coefficient 0.97, indicating very high agreement with the ground truth.

Table 1: Confusion Matrix for ML Classification.

Overall Accuracy = 97.4%
Kappa Coefficient = 0.97

		Ground Truth (Pixels)											
Class		Coastal swamp forest	Dryland forest	Oil palm	Rubber	Cleared land	Sediment plumes	Water	Coconut	Bare land	Urban	Industry	Total classified pixels
ML Classification (pixels)	Coastal swamp forest	14801	0	0	0	0	0	1	0	0	0	0	14802
	Dryland forest	0	6116	3	1	0	0	0	0	0	0	0	6120
	Oil palm	0	9	9690	0	18	0	0	8	0	0	0	9725
	Rubber	0	24	0	102	4	0	0	0	0	0	0	130
	Cleared land	0	4	111	0	1173	3	0	0	0	123	1	1415
	Sediment plumes	33	2	12	0	9	1804	0	4	0	0	0	1864
	Water	0	0	0	0	0	0	9119	0	0	0	0	9119
	Coconut	0	5	672	0	8	74	0	147	0	0	0	906
	Bare land	0	0	0	0	4	0	0	0	313	0	0	317
	Urban	0	0	4	0	11	0	0	0	0	2154	0	2169
	Industry	6	2	0	0	23	0	9	0	0	32	349	421
	Total ground truth pixels	14840	6162	10492	103	1250	1881	9129	159	313	2309	350	46988

(a)

Class	Producer Accuracy		User Accuracy	
	(Pixels)	(%)	(Pixels)	(%)
Coastal swamp forest	14801/14840	99.74	14801/14802	99.99
Dryland forest	6116/6162	99.25	6116/6120	99.93
Oil palm	9690/10492	92.36	9690/9725	99.64
Rubber	102/103	99.03	102/130	78.46
Cleared land	1173/1250	93.84	1173/1415	82.90
Sediment plumes	1804/1881	95.91	1804/1864	96.78
Water	9119/9129	99.89	9119/9119	100.00
Coconut	147/159	92.45	147/906	16.23
Bare land	313/313	100.00	313/317	98.74
Urban	2154/2309	93.29	2154/2169	99.31
Industry	349/350	99.71	349/421	82.90

(b)

3.3 Correlation Matrix Analysis

Classification uses the covariance of the bands; nonetheless, covariance is not intuitive; more intuitive is correlation, $\rho_{k,l}$, i.e. covariance normalised by the product of the standard deviations of bands, k and l :

$$\rho_{k,l} = \frac{C_{k,l}}{\sigma_k \sigma_l} = \frac{E((I_k - \mu_k)(I_l - \mu_l))}{\sigma_k \sigma_l} \quad (15)$$

where $C_{k,l}$ is the covariance between bands k and l , σ_k and σ_l are the standard deviations of the measurements in bands k and l respectively, E is the expected value operator, and I_k and I_l and μ_k and μ_l are the intensities and means of bands k and l respectively. When using more than two bands, it is convenient to use a correlation matrix, where the element in row m and column n that correspond to band k and l is given by $\rho_{k,l}$. If $m = n$, then $\rho_{k,l} = 1$, so this will be the value of the diagonal elements of the matrix. Otherwise, if $m \neq n$, $\rho_{k,l}$ lies between -1 and 1 . In order to analyse the correlation matrices, plots of correlation versus band pair for all classes are plotted. Figure 3 shows correlation between band pairs from selected classes, i.e. (a) water, (b) coastal swamp forest, (c) dryland forest, (d) oil palm, (e) urban, (f) cleared land, (g) industry and (h) sediment plumes. Each coloured curve represents correlation between a specific band (given by a specific colour) with all bands (on the x-axis). Landsat bands 1, 2 and 3 are located within a very close wavelength range of the visible spectrum, with their centre wavelengths differing only by about $0.1 \mu\text{m}$. Measurements made from these bands normally exhibit similar responses and therefore are highly correlated. Poor correlations may result from mixed pixel problem

(existence of more than one class in a pixel). Correlations between lower-numbered bands (i.e. bands 1, 2 and 3) and higher-numbered bands (i.e. bands 4, 5, and 6) are much lower because involving non-adjacency wavelengths. From Figure 3, for cleared land and sediment plumes, correlation in most band pairs is quite high in ML, especially for bands 1, 2 and 3, which corresponds to the higher accuracy in these classes in ML. For certain classes, such as water (with very low reflectances), the superiority of ML is even clearer, as shown not only by the correlations from bands 1, 2 and 3, but also 4, 5 and 7 in ML that have high correlations. A high correlation is shown by industry (with very high reflectances) due to the strong relationships of variation between the brightness of pixels and mean brightness in all bands (1, 2, 3, 4, 5 and 7).

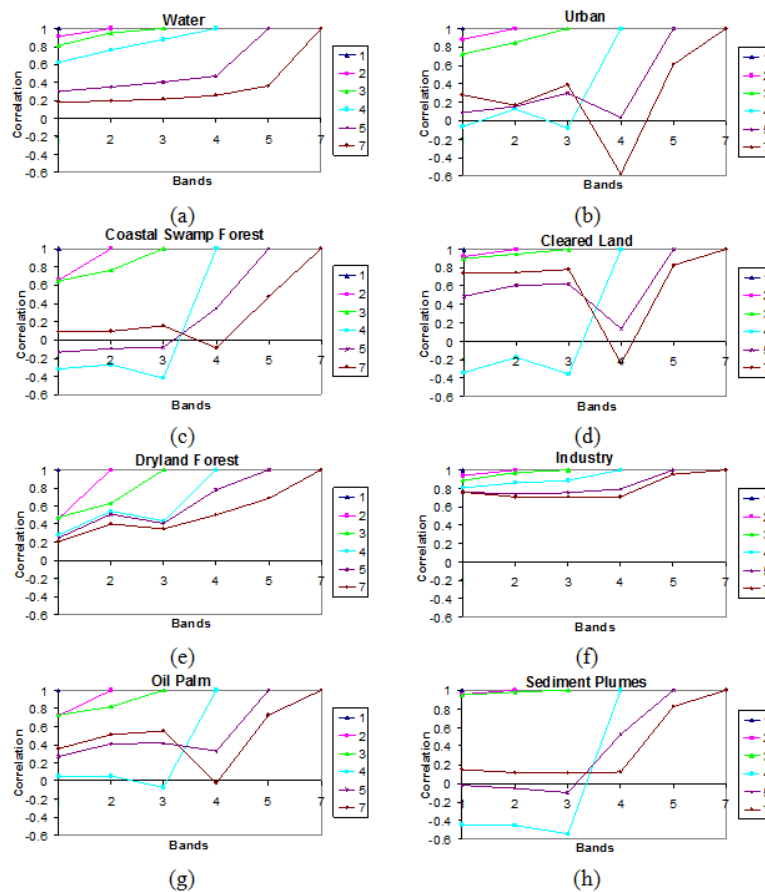


Fig. 3. Correlations between band pairs for (a) water, (b) coastal swamp forest, (c) dryland forest, (d) oil palm, (e) urban, (f) cleared land, (g) industry and (h) sediment plumes.

3.4 Mean, Standard Deviation and Decision Boundary Analysis

Despite of being very similar, both forests can still be separated quite effectively from each other using ML. Here, we investigate further the forests in terms of

mean, standard deviation and decision boundary. Figure 4(a) shows the means and (b) standard deviation of coastal swamp forest and dryland forest classes in ML. The means are almost the same particularly in bands 1, 2 and 3. The standard deviation of coastal swamp forest is bigger than dryland forest in most of the bands, except band 5.

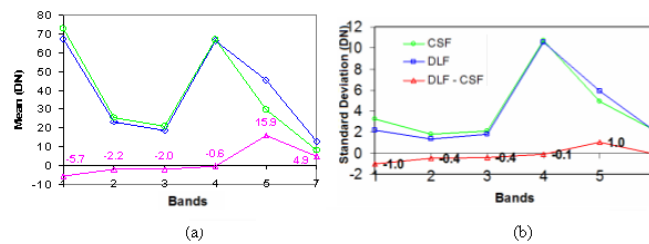


Fig. 4. (a) Means of coastal swamp forest and dryland forest classes in ML classification. DLF and CSF are dryland forest and coastal swamp forest respectively. (b) Standard deviations of the coastal swamp forest and dryland forest classes in ML classification

We subsequently generated the decision boundaries using Equation (10) between coastal swamp forest and dryland forest. Figure 5 shows 15 sets of decision boundaries; 'M1' and 'M2' are the means for dryland forest and coastal swamp forest respectively, 'Band k Vs. Band l' denotes that the vertical axis is band k while horizontal axis is band l and 'CSF' and 'DLF' indicate coastal swamp forest and dryland forest respectively. The decision boundaries formed by the ML have the form of conic sections, i.e. pairs 2:1, 3:1, 7:1, 3:2 and 7:2 form an elliptic curve, pairs 5:1, 5:2, 5:3, 7:3 and 7:5 form a parabolic curve and pairs 4:1, 4:2, 4:3, 5:4 and 7:4 form a hyperbolic curve. Most of the boundaries are owned by dryland forest swamp forest due to the smaller standard deviation of dryland forest than coastal swamp forest in most of the bands. In most bands (except band 4), the difference between the means is big enough that M1 and M2 are located in the different side of the boundary. Hence, ML can effectively separate between the forests due to its ability in positioning the means in the different side of the decision boundary.

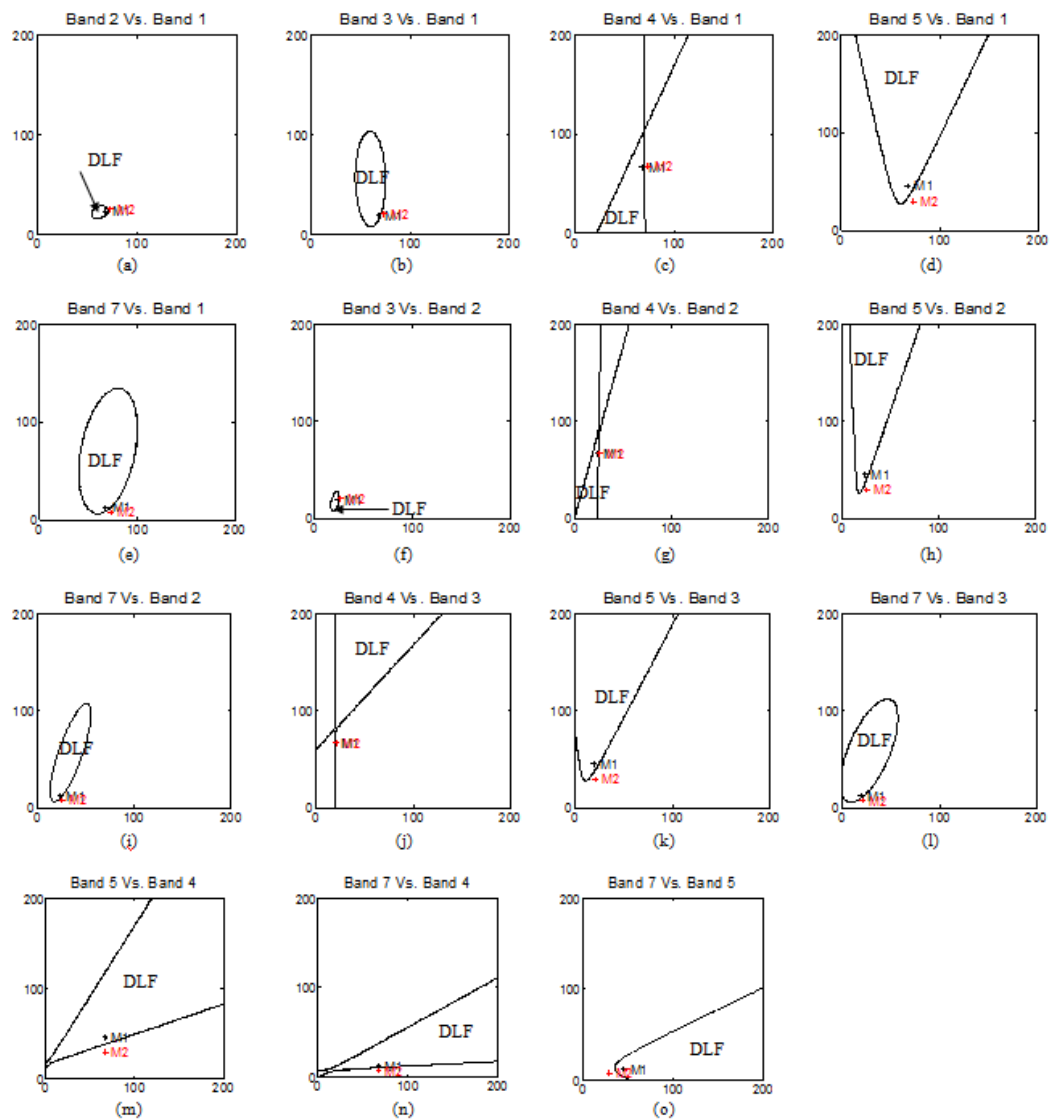


Fig. 5. Decision boundaries between coastal swamp forest and dryland forest for ML classification.

4 Conclusions

In this study, detail analyses of ML classification for tropical land covers in Malaysia have been carried out, in which lead to a number of conclusions. ML classifies the classes that exist in the study area with a good agreement with the reference map. ML classified the study area into 11 classes, with accuracy 97% ($\kappa = 0.97$). ML classifies pixels based on known properties of each cover type, but the generated classes may not be statistically separable. The band correlation of classes with high reflectance, e.g. industry, is high for all band pairs in ML because of the strong relationships of variation between the brightness of pixels

and mean brightness in all bands. The separation between mean of the classes in the decision space is believed to be one of the main factors that leads to the high classification accuracy of ML.

References

- [1] A. Ahmad, and S. Quegan, Cloud masking for remotely sensed data using spectral and principal components analysis, *Engineering, Technology & Applied Science Research (ETASR)*, **2** (2012), 221 – 225.
- [2] ENVI, *User's guide*, Research Systems Inc., USA, 2006.
- [3] J. Scepan, Thematic validation of high-resolution global land-cover data sets, *Photogrammetric Engineering and Remote Sensing*, **65** (1999), 1051 – 1060.
- [4] J.A. Richards, *Remote sensing digital image analysis: An introduction*. Springer-Verlag, Berlin, Germany, 1999.
- [5] J.B. Campbell, *Introduction to remote sensing*, Taylor & Francis, London, 2002.
- [6] J.R. Jensen, *Introductory Digital Image Processing: A Remote Sensing Perspective*, Pearson Prentice Hall, New Jersey, USA, 1996.
- [7] M. Story and R. Congalton, Accuracy assessment: a user's perspective, *Photogrammetric Engineering and Remote Sensing*, **52** (1986), 397 – 399.
- [8] S.A. Ackerman, K.I. Strabala, W.P. Menzel, R.A. Frey, C.C. Moeller and L.E. Gumley, Discriminating clear-sky from clouds with MODIS, *Journal of Geophysical Research*, **103** (1998), 32141 – 32157.
- [9] T.M. Lillesand, R.W. Kiefer and J.W. Chipman, *Remote Sensing and Image Interpretation*, John Wiley & Sons, Hoboken, NJ, USA, 2004.

Received: August, 2012